Trends in inversion barriers. I. Group-15 hydrides

Peter Schwerdtfeger
Department of Chemistry, University of Auckland, Private Bag 92091, Auckland, New Zealand, and the Research School of Chemistry, The Australian National University, G.P.O. Box 4, Canberra, Australian Capital Territory 2601, Australia

Liisa J. Laakkonen[a)] and Pekka Pyykkö
Department of Chemistry, University of Helsinki, Et. Hesperiankatu 4, 00100 Helsinki, Finland

(Received 26 November 1991; accepted 23 January 1992)

Inversion barriers for the group-15 hydrides NH_3, PH_3, AsH_3, SbH_3 and BiH_3 have been studied using *ab initio* self-consistent-field methods including electron correlation and relativistic effects. A modified symmetric inversion potential is introduced to describe the inversion from the minimum C_{3v} arrangement through the D_{3h} transition state. Tunneling rates and frequencies are calculated at the Hartree–Fock and Møller–Plesset (MP2) level within the Wentzel–Kramers–Brillouin approximation. At the MP2 level the calculated $0^+/0^-$ ν_2 frequency splitting of the vibronic ground state of NH_3/ND_3 ($0.729\ \mathrm{cm}^{-1}/0.041\ \mathrm{cm}^{-1}$) is in excellent agreement with the experimental values ($0.794\ \mathrm{cm}^{-1}/0.053\ \mathrm{cm}^{-1}$). The tunneling rate for PH_3 suggests that previously published values are wrong by orders of magnitude. Correlation effects do not change the barriers significantly in accordance with Freed's theorem. This has been studied in more detail for BiH_3 at the quadratic configuration-interaction (QCI) level. Relativistic effects increase the barrier height of BiH_3 by 81.6 kJ/mol at the QCI level. Nonrelativistic and relativistic extended Hückel calculations suggest that the a_1 highest occupied molecular orbital, which is antibonding to the Bi 6*s*, relieves part of its antibonding character near equilibrium geometry due to the relativistic radial contraction of the 6*s* orbital and hence increases the barrier height. In the planar transition state this orbital is a nonbonding a_2''. The increasing trend in barrier heights from NH_3 to BiH_3 can be explained by a second-order Jahn–Teller distortion of the trigonal planar geometry. Vibrational frequencies are predicted for BiH_3.

I. INTRODUCTION

Pyramidal atomic inversion normally involves a passage through a transition state, in which the molecule possesses a local D_{nh} symmetry if all n ligands are equivalent.[1–7] This is, for example, the case for the group-15 hydrides[2,3] MH_3 with M = N, P, As, or Sb and for NF_3.[8] In the inversion process the lone pair at the central atom turns from "sp^3" in the bent arrangement to a pure *p* orbital in the transition state. Dixon and co-workers[9–14] recently showed that some of the group-15 fluorides rather prefer a T-shaped transition structure with an F–M–F angle of almost 90°. The heaviest element in this series, bismuth, has not been studied extensively and the transition-state structures of the BiL_3 inversion are unknown.[15,16] Relativistic effects may contribute strongly to the structures and energy barriers of BiH_3, since the relativistic stabilization of the 6*s* orbital is quite large in bismuth and *s* participation plays an important role in the inversion process.[1] This has been shown recently by one of us in a semiempirical relativistic (R) vs nonrelativistic (NR) extended Hückel study (REX and EHT, respectively)[17] of MH_3 (M = N,...,Bi), and is reported below.

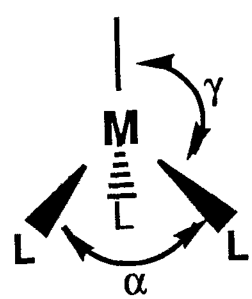

It is well known that the barrier height in the inversion of the group-15 hydrides NH_3 to SbH_3 increases with decreasing H–M–H angle α (Fig. 1).[1] This has been rationalized by several authors using simple molecular orbital (MO) pictures.[3,4,18–21] The barrier height increases sharply from NH_3 to PH_3 but varies only slightly from PH_3 to BiH_3, (Fig. 2).[21] It is widely accepted that electronegative ligands increase the inversion barrier.[3,22–25] However, comparing the data given by Clotet, Rubio, and Illas[8] and Dixon and co-workers[9–13,26,27] suggests that the fluorides along the series NF_3 to SbF_3 follow the reverse trend compared to the hydrides. This is shown in Fig. 2. The reason for this behavior is not immediately understood and is not related to the

[a)] Present address: Department of Physiology and Biophysics, Mount Sinai School of Medicine, City University of New York, New York, NY 10029.

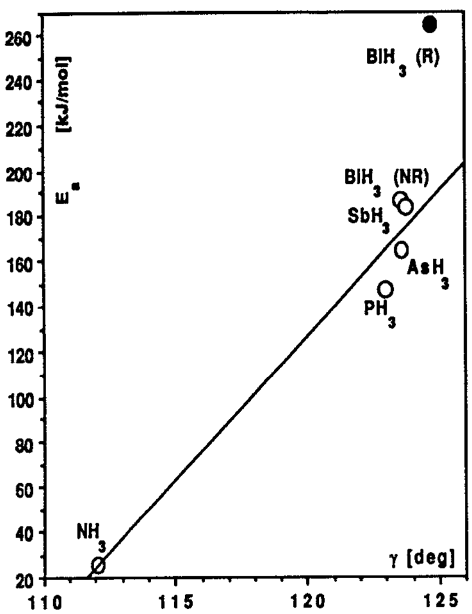

FIG. 1. MP2 inversion barriers E_a vs bonding angle γ for the group-15 hydrides ($\gamma = 90°$ is defined as the planar MH_3 arrangement).

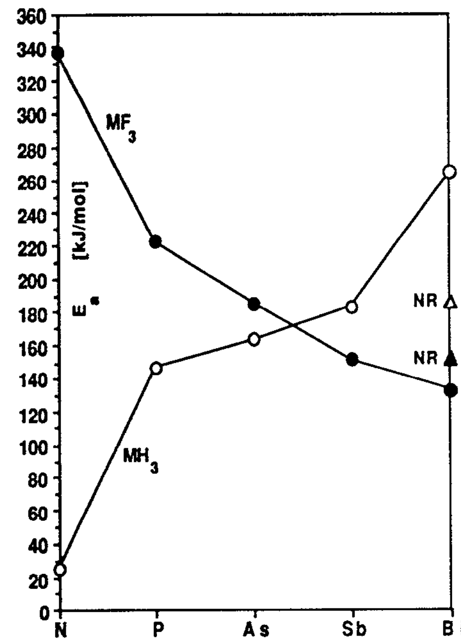

FIG. 2. MP2 inversion barriers for the group-15 hydrides MH_3 and fluorides MF_3 (M = N, P, As, Sb, and Bi). The values for the group-15 fluorides are taken from Ref. 25.

unusual transition states of the fluorides.[25] Hence, trends in barrier heights along the series N, P, As, Sb, and Bi cannot be explained by simply using the H–M–H angles.

For calculating tunneling frequencies ν_T and tunneling rates τ_T of the MH_3 molecules, the shape of the inversion potential has to be known. However, the calculation of the potential-energy curve can become quite expensive in computer time, especially for systems containing heavier atoms, when correlation and relativistic effects are taken into account. Moreover, most formulas for symmetric double-well potentials, which are easy to adjust to calculated or experimental values, are quite inaccurate and often do not represent very well the calculated one-dimensional inversion potentials. As a result, published tunneling rates differ often by orders of magnitude depending on the approximation used. For example, tunneling rates for AsH_3 published so far lie between 53 s and 1.4 years.[28–31] It is therefore desirable to find a suitable but accurate functional form describing the inversion process, which contains some simple adjustable parameters. This is certainly useful for *ab initio* calculations of accurate tunneling rates of more general MR_3 molecules (R, for example, an organic substituent) in order to evaluate whether optically active compounds may exist on an experimental time scale.

In this paper we present simple but straightforward REX/EHT analysis of trends and relativistic effects on the MH_3 (M = N,...,Bi) inversion barriers and compare the results with credible *ab initio* calculations using quasirelativistic (QR) pseudopotentials (PP) for the heavier elements. We introduce a modified symmetric Gaussian barrier for computing tunneling rates within the Wentzel–Kramers–Brillouin approximation (WKB). The methods used are described in detail in the next section. Results and discussion are presented in Sec. III. A summary is given in Sec. IV.

II. METHODS

A. REX calculations

The calculations were carried out using the ITEREX-87 program[32] (and consumed about 10 s of PC time/point).[17] The default parameters[33] were used for the group-15 atoms. The hydrogen parameters were taken as $\alpha_H = -10$ eV (Ref. 34) and $\zeta_H = 1.3$. The M–H distances were kept fixed at 1.02, 1.41, 1.51, 1.71, and 1.79 Å for N, P, As, Sb, and Bi, respectively. The Bi–H distance was estimated, the other distances were experimental.[35] The experimental H–M–H angles α (107.6°, 93.6°, 92.0°, and 91.6°) were used for N to Sb, respectively. For Bi, the difference between 90° and 120° is discussed below.

B. *Ab initio* calculations

The quantum-chemical program packages GAUSSIAN88[36] and TURBOMOLE[37–39] have been used for all calculations. The geometries are optimized at the Hartree–Fock (HF) as well as the correlated level of theory [Møller–Plesset perturbation theory of second order (MP2)]. BiH_3 has been investigated at the MP3, MP4, and the quadratic configuration-interaction level (QCI) including triples corrections,[40–42] which is known to perform extremely well compared to other correlation procedures.[43] For H we took a contracted Huzinaga $(9s)/[6s]$ basis set[44] with two p-polarization functions given by Lie and Clementi[45] and a diffuse s function with exponent 0.01. Trucks *et al.*[46] pointed out that for an accurate description of the ν_2 (A_1) bending mode of NH_3 large basis sets are needed. Therefore, for N and P a 6-311 + G* basis set was taken,[36,47] but these basis sets have been decontracted to a 6-2111 + G* set to allow more flexibility in s–p mixing for the inversion process. For As we took a Binning–Curtiss (6111111111s/611111p/411d) basis set[48] including diffuse functions with exponents 0.021 for s and p, and 0.273 for d. For Sb and Bi we applied energy-adjusted pseudopotentials[49,50] since relativistic effects have to be included for the heavier atoms. For Sb we took a (7s/5p/1d) basis set[25] with d exponent 0.211.[45] For Bi a nonrelativistic (NR) and relativistic (R) (7s/6p/1d) basis set[50] with d exponent 0.17 (Ref. 51) was taken. The force constants are defined according to Wilson, Decius, and Cross.[52] The harmonic generalized force fields have been obtained using the program VIB,[53] which fits the force field to fundamental frequencies according to Wilson's GF matrix method.

C. The inversion potential

We use a modified symmetric Gaussian barrier for all inversion potentials,

$$V(x)=(a+bx^2+cx^4)e^{-dx^2},\quad -|x_{\min}|\leqslant x\leqslant|x_{\min}| \tag{1}$$

with the boundary conditions $V(x_{\min})=0$, $x_{\max}=0$, and $V(x_{\max})=E_a$. This leads to simple formulas for the coefficients a, b, c, and d,

$$a=E_a,\quad b=-\frac{2E_a}{x_{\min}^2},\quad c=\frac{E_a}{x_{\min}^4}. \tag{2}$$

The fourth coefficient d will be chosen to fit one point of the potential curve lying in the region between $x_{\min}$ and $x_{\max}$, which we denote as $x_{1/2}$ ($d=-x_{1/2}^{-2}\times\ln[V(x_{1/2})\cdot(a+bx_{1/2}^2+cx_{1/2}^4)^{-1}]$). In order to obtain the adjustable parameters of Eq. (1), the following steps for calculating the tunneling splitting for the ground-state vibrational level have to be performed ($x=\gamma-90°$):

(1) Calculate the minimum geometry of the ML_3 molecule to find $\gamma_{\min}$ and the L–M–L bending mode frequency $\nu_0(=0\nu_2)$.

(2) Calculate the transition-state geometry ($\gamma=90°$) and the barrier height E_a.

(3) Take the midpoint $\gamma_{1/2}=\gamma_{\min}/2+45°$ and optimize the M–L bond distances at $\gamma_{1/2}$ to obtain $E(\gamma_{1/2})$.

(4) Calculate the coefficients a, b, c, and d of Eq. (1) and perform a numerical integration to obtain the tunneling frequency ν_T and the tunneling rate $\tau_T=(2\nu_T)^{-1}$ by using the well-known WKB formula[54] for symmetric barriers,[28,29,55]

$$\nu_T=\frac{\nu_0}{\pi}e^{\sqrt{\mu}I} \tag{3}$$

with the integral

$$I=-\frac{\sqrt{2}}{\hbar}\int_{-s_0}^{s_0}[V(s)-E_0]^{1/2}ds \tag{4}$$

and the tunneling coordinate s,

$$s=r\cos(180°-\gamma). \tag{5}$$

r denotes the M–H bond distance, μ the effective mass of the ML_3 molecule,

$$\mu=3m_Mm_L(m_M+3m_L)^{-1} \tag{6}$$

and

$$s_0=r[\cos(180°)-\gamma_0],$$
$$\gamma_0=\gamma_{\min}+|\gamma(E_0)-\gamma_{\min}|. \tag{7}$$

$\gamma(E_0)$ is the angle γ at the energy E_0, which can be obtained from Eq. (1). Note that only three geometry optimizations at the three different angles, $\gamma_{\min}$, $\gamma=90°$ and $\gamma_{1/2}$ are necessary to obtain an accurate potential curve for the inversion process. For calculating the integral I [Eq. (4)] we performed a numerical integration using the extended Simpson formula with a mesh of 2000 points between $\gamma(E_0)$ and $\gamma=90°$.[52] The M–H bond distance r changes slightly with changing angle γ, the difference in bond distances between the minimum structure and the inversion state is between 0.01 and 0.09 Å depending on the atomic center M (the difference increases from M = N to M = Bi; Table I). Therefore, for calculating the tunneling coordinate s we took that change into account by using a linear correlation between s and r (nonrigid bender approach[55]). We also included a correction for the angle dependence of the reduced mass, i.e., $\mu(\gamma)=\mu(1+3m_L\sin^2(\gamma-90°)/m_M)$,[53,56] μ as defined in Eq. (6). We should remark that there are more sophisticated analytical formulas available in literature,[57] like those by Manning,[58] Chan *et al.*,[59] Campoy, Palma, and Sandoval,[60] or Papousek and co-workers,[55,61] which, in contrast to ansatz (1), describe the repulsive outer part of the inversion potential quite accurately and are therefore more useful for solving the vibronic Schrödinger equation. However, these formulas do not lead to simple relations for the adjustable coefficients like those in Eq. (1). Also, the coefficients a, b, c, and d of Eq. (1) have simple physical interpretations; the adjustable parameter d, for example, is a measure of the deviation from a simple polynomial behavior,

$$V(x)=a+bx^2+cx^4. \tag{8}$$

Moreover, the vibronic Schrödinger equation for a one-dimensional double-well potential is normally solved by numerical techniques,[30] and for this purpose an additional potential for the repulsive part may be added to ansatz (1). It has also been shown by Papousek and co-workers[62] that the WKB approximation is excellent compared to the numerical solution of the Schrödinger equation, especially in lower regions of the inversion potential. Hence, the errors introduced by the various approximations used within the *ab initio* procedure are expected to be large compared to the inaccuracy of the WKB approximation. Moreover, for very small inversion splittings the numerical solution of the Schrödinger equation becomes extremely difficult and the WKB approximation seems to be the only available accurate method to calculate small frequency splittings.

III. RESULTS AND DISCUSSION

A. Molecular properties

The calculated geometries at the MP2 level for the group-15 hydrides are all in excellent agreement with experimental values (Table I). In most cases the accuracy in the calculated M–H bond distance is better than 0.01 Å. For

TABLE I. Molecular properties for MH_3 compounds ($M = N$ to Bi). M–H bond distances r_e in Å, angles γ_e in deg, dipole moments μ_e in D, and barrier height E_a in kJ/mol. r_e^T denotes the M–H bond distance at the trigonal planar transition state. Experimental geometries and dipole moments are from Refs. 63 and 64, respectively. The signs in front of the experimental dipole moments are assumed. NR values are set in parentheses.

		r_e	γ_e	μ_e	r_e^T	E_a
N	HF	1.000	111.22	−1.60	0.986	22.0
	MP2	1.011	112.05	−1.56	0.995	25.1
	Expt.	1.012	112.14	(−)1.471		(24.2)[a]
P	HF	1.412	121.35	−0.76	1.376	150.2
	MP2	1.413	122.98	−0.61	1.375	146.8
	Expt.	1.420	122.86	(−)0.578		(132)[b]
As	HF	1.510	122.10	−0.45	1.461	171.1
	MP2	1.509	123.61	−0.35	1.457	164.0
	Expt.	1.511	123.78			
Sb	HF	1.688	122.43	0.14	1.630	192.5
	MP2	1.692	123.80	0.33	1.633	183.5
	Expt.	1.704	124.1	(+)0.116		
Bi	HF	1.806 (1.825)	123.45 (122.44)	1.44 (0.46)	1.715 (1.763)	271.5 (194.8)
	MP2	1.809 (1.827)	124.70 (123.59)	1.48 (0.62)	1.721 (1.764)	264.2 (186.5)

[a] Reference 6.
[b] Reference 5.

NH_3 the MP2 geometry is in good agreement with MP2 results published by Simandiras, Handy, and Amos ($r_e = 1.009$ Å, $\gamma_e = 111.71°$),[65] who used extensive basis sets for both the nitrogen and the hydrogen atom. Experimental data for gas-phase BiH_3 are not available. However, we can compare our QCI bond distance (1.826 Å; Table II) with a complete-active-space self-consistent-field second order configuration-interaction (CASSCF/SOCI) value by Dai and Balasubramanian[16] (1.865 Å). Table II shows that electron correlation increases the Bi–H bond length by maximal 0.02 Å. Hence the difference of our QCI bond length with the CASSCF/SOCI value of about 0.04 Å for BiH_3 is probably due to differences in the pseudopotentials and basis sets used. For NH_3 an accurate experimental value for the (effective) barrier height E_a has been published [24.2 kJ/mol (Ref. 6)], which is in excellent agreement with our calculated MP2 value (25.1 kJ/mol). Near HF limit calculations[66–69] suggest that the correlation contribution to the barrier height is small and of ca. 2.5 kJ/mol, which is close to our MP2 value (3.1 kJ/mol), but larger than a coupled-electron-pair approximation (CEPA) value given by Ahlrichs *et al.*[70] (1.7 kJ/mol). Less close agreement, however, is obtained for the PH_3 molecule if we compare our MP2 value (146.8 kJ/mol; Table I) with an experimentally estimated barrier height [132 kJ/mol (Ref. 5)], but we like to point out that it is difficult to estimate high activation barriers on an experimental basis. Moreover, our value is in agreement with a previously published result by Ahlrichs *et al.*[71] (145.8 kJ/mol) or Marynick and Dixon[72] (143.9 kJ/mol). We therefore conclude that the MP2 values are encouraging for calculating inversion barriers.

To investigate the role of electron correlation in more detail we performed MP3, MP4, and QCI calculations for the least-studied molecule so far, BiH_3. The results are presented in Table II. The BiH_3 inversion barriers at different levels of electron correlation do not vary much. This is in

TABLE II. Molecular properties for BiH_3 at various levels of the theory. Bi–H bond distances r_e in Å, H–Bi–H bond angles α_e in deg, symmetric stretching force constants k_e (per Bi–L bond) in mdyn Å^{-1}, and the barrier height E_a in kJ/mol. T denotes the molecular properties at the trigonal planar transition state. NR values are set in parentheses.

	HF	MP2	MP3	MP4	QCI
BiH_3 r_e	1.806 (1.825)	1.809 (1.826)	1.816 (1.831)	1.820 (1.835)	1.826 (1.839)
α_e	92.5 (93.9)	90.8 (92.2)	90.7 (92.0)	90.8 (92.0)	90.7 (91.9)
k_e	2.13 (2.28)	2.03 (2.17)	1.96 (2.13)	1.92 (2.09)	1.85 (2.03)
BiH_3 r_e^T	1.715 (1.763)	1.721 (1.764)	1.727 (1.769)	1.730 (1.772)	1.735 (1.775)
(D_{3h}) k_e^T	2.76 (2.77)	2.56 (2.65)	2.47 (2.57)	2.42 (2.53)	2.33 (2.47)
E_a	271.5 (194.8)	264.2 (186.5)	268.5 (189.0)	270.9 (190.9)	270.6 (189.0)

accordance with electron correlation studies on NH_3.[73] In fact, the NR and R HF values are close to the QCI results in agreement with Freed's theorem.[74] Therefore, HF describes accurately the barrier height despite the fact that the barrier height itself is quite large.[75] Electron correlation contributions to E_a vary between 3.1 kJ/mol (NH_3) and -9.0 kJ/mol (SbH_3) at the MP2 level. Note that except for NH_3 electron correlation lowers the barrier height. Table II also demonstrates that the MP2 approximation is sufficient for obtaining good inversion barriers.

In Table III calculated frequencies are listed in comparison with experimental results. The 6-2111 + G* basis set for N performs extremely well, i.e., for NH_3 our HF harmonic frequencies are in very good agreement with values published recently by Amos ($\nu_1 = 3691$ cm^{-1}, $\nu_2 = 1099$ cm^{-1}, $\nu_3 = 3815$ cm^{-1}, $\nu_4 = 1787$ cm^{-1}),[84] who used basis sets of HF-limit quality. For an accurate description of the ν_2 bending mode a CI with very large basis sets is required.[46] However, our MP2 value for the ν_2 mode (1069 cm^{-1}; Table III) is in good agreement with the estimated harmonic experimental frequency (1022 cm^{-1}).[76]

Table IV shows the adjusted force field including off-diagonal elements. In all cases the fit procedure yields the exact input frequencies. Several local and global minima with quite different off-diagonal force constants appeared in the fit procedure. Most of these off-diagonal force constants are relatively small, but essential for obtaining a satisfying fit to given frequencies. Off-diagonal force constants can be very sensitive to basis-set effects and to the method of electron correlation applied. We therefore chose the fit which kept the off-diagonal elements as small as possible. This distinguishes our force fields from first-principle *ab initio* determined force fields which may show larger off-diagonal force constants. HF and MP2 M–H stretching and H–M–H bending force constants are overestimated (by about 10% at the MP2 level) compared to results obtained from fitting experimental frequencies. We therefore chose a scaling factor of $f_S = 0.9$ for BiH_3 (Table IV) using the MP2 off-diagonal force constants to predict the fundamental frequencies for this molecule (Table III), which are unknown.

TABLE III. Vibrational frequencies ν in cm^{-1} and infrared intensities in 10^3 m/mol (set in parentheses behind the wave numbers) for the MH_3 compounds in C_{3v} symmetry (M = N to Bi). If not otherwise indicated, HF and MP2 refer to NRHF and NRMP2, respectively. Experimental frequencies from Refs. 76–80. Experimental intensities for NH_3 from Ref. 81. The frequencies for ND_3 (D = deuterium) are calculated using the NH_3 force field of Table IV.

Molecule		$\nu_1(A_1)$	$\nu_2(A_1) = \nu_0$	$\nu_3(E)$	$\nu_4(E)$
NH_3	HF	3692(0.8)	1123(184)	3817(6)	1795(19)
	MP2	3524(3)	1069(148)	3672(6)	1710(14)
	Harm.[a]	3506	1022	3577	1691
	Expt.	3336(8)[b]	950(138)[b]	3414(4)	1628(32)
ND_3	HF	2664	875	2820	1301
	MP2	2543	809	2717	1250
	(Expt.ff)[c]	2401	719	2524	1192
	Expt.	2419	749	2555	1191
PH_3	HF	2520(43)	1099(31)	2519(92)	1232(20)
	MP2	2468(39)	1036(28)	2474(67)	1179(17)
	Expt.	2321[d]	991[b]	2327[d]	1121
AsH_3	HF	2317(84)	1008(44)	2317(151)	1108(22)
	MP2	2248(74)	941(35)	2262(110)	1053(17)
	Expt.	2122	906	2185	1005
SbH_3	RHF	2084(131)	903(115)	2074(232)	946(37)
	RMP2	2023(119)	834(87)	2022(182)	887(29)
	Expt.	1891	782	1894	831
BiH_3	HF	1978(181)	816(146)	1967(291)	840(45)
	MP2	1927(169)	755(111)	1922(235)	785(35)
	RHF	1904(309)	835(81)	1903(409)	846(23)
	RMP2	1857(253)	759(56)	1863(298)	780(16)
	Predicted[e]	1760	720	1770	750

[a] Due to strong anharmonicity effects the $0 \rightarrow 1$ transitions are substantially different from the (experimental) harmonic frequencies given in Ref. 76.
[b] Averaged over Fermi resonance splitting.
[c] expt.ff: Calculated frequencies for ND_3 using the NH_3 force field obtained from experimental frequencies (Table IV).
[d] The often used frequencies for the ν_1 (2327 cm^{-1}) and ν_3 (2421 cm^{-1}) mode of gas-phase PH_3, for example, given in Nakamoto (Ref. 79) or Corbridge (Ref. 82), are those of Lee and Wu from 1939 (Ref. 83) and should be replaced by the frequencies published in Refs. 77 and 78.
[e] The predicted BiH_3 frequencies include anharmonicity effects.

TABLE IV. HF and MP2 and adjusted experimental force constants for the group-15 hydrides (in mdyn/Å). $k'_{r\alpha}$ is the off-diagonal force constant between the M–H bond and the adjacent HMH plane.

Molecule	Method	k_r	k_α	$k_{rr'}$	$k_{\alpha\alpha'}$	$k_{r\alpha}$	$k'_{r\alpha}$
NH_3	HF	7.895	0.677	−0.012	−0.056	0.002	0.001
	MP2	7.251	0.615	−0.060	−0.064	−0.093	0.068
	Expt.	6.364	0.536	0.028	−0.078	0.040	−0.011
PH_3	HF	3.639	0.419	0.001	−0.003	0.170	0.018
	MP2	3.514	0.368	0.003	−0.025	0.002	0.009
	Expt.	3.102	0.336	−0.005	−0.020	−0.045	0.009
AsH_3	HF	3.141	0.343	−0.002	−0.009	0.089	0.007
	MP2	2.982	0.306	−0.013	−0.012	0.075	0.009
	Expt.	2.742	0.279	−0.054	−0.009	0.055	0.026
SbH_3	HF	2.532	0.262	0.002	0.004	0.094	−0.003
	MP2	2.399	0.229	−0.007	0.003	0.094	0.003
	Expt.	2.099	0.203	−0.011	0.004	0.094	−0.005
BiH_3 (NR)	HF	2.284	0.211	0.001	0.007	0.091	−0.004
	MP2	2.173	0.185	−0.007	0.007	0.098	0.002
BiH_3 (R)	HF	2.130	0.216	−0.008	0.010	0.087	0.001
	MP2	2.033	0.185	−0.015	0.008	0.095	−0.003
	Scaled	1.83	0.17	−0.015	0.008	0.095	−0.003

Figure 3 shows k_r and k_α for the whole series from NH_3 to BiH_3. Both force constants decrease monotonically from NH_3 to BiH_3, as expected. The irregularity in the bending mode frequency from NH_3 (950 cm^{-1}) to PH_3 (991 cm^{-1}) no longer shows up in the force constants. Due to very strong anharmonicities in the NH_3 bending potential curve the $0\rightarrow 1$ $\nu_2(A_1)$ transition is 64 cm^{-1} above the $0\nu_2(A_1)$ ground-state vibrational level (886 cm^{-1}). PH_3 is expected

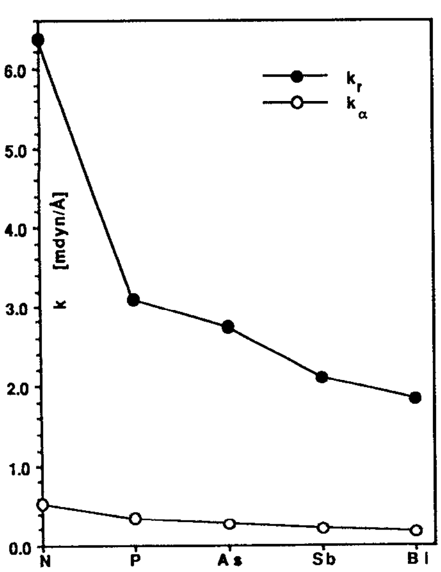

FIG. 3. MP2 M–H stretching and H–M–H bending force constants for the group-15 hydrides.

to show smaller anharmonicity effects compared to NH_3 due to the larger barrier height of the PH_3 inversion, i.e., compare the difference of the calculated MP2 frequencies to the experimental $0\rightarrow 1$ transitions (Table I) for NH_3 (119 cm^{-1}) and PH_3 (60 cm^{-1}). This makes a harmonic frequency analysis using only second derivatives of the total energy questionable. However, the calculated frequencies for ND_3 using the force field obtained from experimental frequencies of NH_3 which include anharmonicity effects are in very good agreement with measured results (Table III). Moreover, harmonic frequencies adjusted from experimental frequencies are available for NH_3,[76] and are in good agreement with our MP2 values (Table III).

The HF infrared intensities for NH_3 (Table III) are in reasonable agreement with near HF-limit results of Amos.[84] The trends in the MP2 infrared intensities are depicted in Fig. 4. There is an increasing trend in the intensities of all four modes from NH_3 to BiH_3, except for the ν_2 modes of NH_3 and BiH_3 and the ν_4 mode of BiH_3. In the case of BiH_3 this is related to relativistic effects, i.e., compare the NRMP2 and RMP2 values given in Table III. For MH_3 the measured $0\rightarrow 1$ $\nu_2(A_1)$ frequencies also show an irregularity from M = N to M = P; however, the ν_2 frequency is *increasing* from NH_3 to PH_3. Hence, the high intensity of the NH_3 $0\rightarrow 1$ ν_2 transition compared to PH_3 must be due to the change of the dipole moment in the symmetric bending which deserves more detailed investigation. Perhaps the very large (absolute value of the) dipole moment plus the relatively small bonding angle of NH_3 compared to PH_3 is responsible for the intense ν_2 mode. Note that the intensities of the symmetric stretching modes are above the antisymmetric ones in contrast to the bending modes.

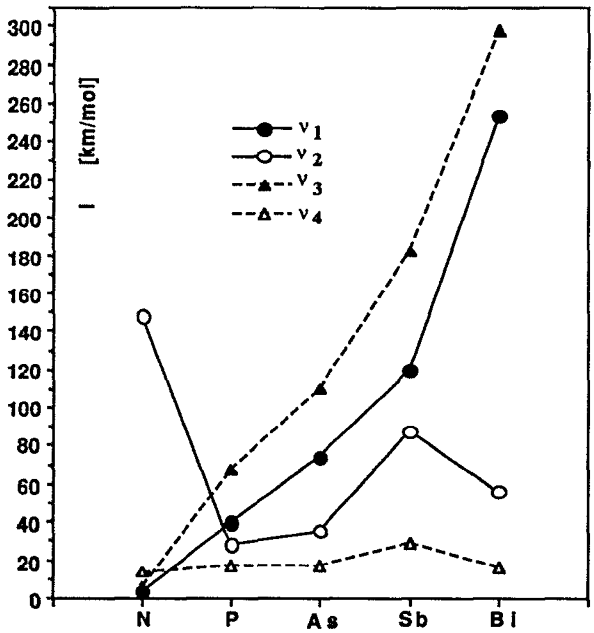

FIG. 4. MP2 infrared intensities for the A_1 modes (ν_1, ν_2: solid lines) and E modes (ν_3, ν_4: dashed lines) of the group-15 hydrides.

Relativistic effects in the BiH_3 force field are relatively small and within the accuracy of our chosen methods (for a detailed discussion of relativistic effects in the main group hydrides and along the sixth period see Refs. 85 and 86). Figure 5 indicates that the NR and R potential curves are similar in shape around the minimum, the R curve being shifted to a slightly smaller angle γ (for the region $\gamma < 90°$).

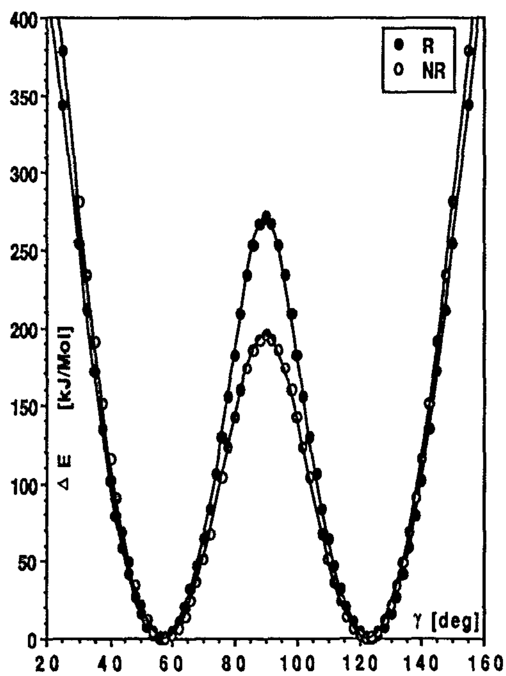

FIG. 5. Nonrelativistic and relativistic HF inversion potential curves $\Delta E(\gamma)$ of BiH_3.

The only larger relativistic change occurs in the BiH_3 dipole moment ($\Delta_R\mu = -0.9$ D). The dipole moments increase monotonically from NH_3 ($\mu = -1.56$ D) to BiH_3 ($\mu = +1.48$ D), in accordance with the increase in the gross atomic charges q obtained by a Mulliken population analysis (Table VI), i.e., for NH_3 we have $q_N = -0.60$ increasing to $q_{Bi} = +1.04$ for BiH_3. This can be rationalized as being due to the decreasing electronegativity from nitrogen down to bismuth.

The inversion barriers of pyramidal ML_3 and ML_4 molecules have been reviewed by Boldyrev and Charkin.[21] The trend in the inversion barrier heights E_a is shown in Figs. 1 and 2, and is almost linear with respect to the angle γ (taking the NR value for BiH_3), $E_a(\gamma) = 12.793\gamma - 1409$ (kJ/mol). The common explanation for this increase is that the H–M–H angle α is decreasing along the series NH_3, PH_3, AsH_3, SbH_3, and BiH_3, i.e., the larger the deviation $\Delta\alpha$ from the planar D_{3h} structure the higher the barrier height E_a.[1] The decreasing trend in the L–M–L bond angles from M = N to M = Bi is consistent for both the hydrides (L = H) and fluorides (L = F) and may be explained in terms of simple models.[87,88] However, the barrier heights and L–M–L bond angles do not seem to be related in a transparent way. The trend in barrier heights with decreasing L–M–L angle shows the reverse behavior for the fluorides compared to the hydrides (Fig. 2). As a consequence, SbF_3 and BiF_3 have lower barrier heights than SbH_3 and BiH_3, respectively. Hence, electrostatic models, as used for example in Ref. 21, are not adequate. We can rationalize this trend by applying a pseudo–Jahn–Teller (JT) symmetry breaking of the D_{3h} into the C_{3v} structure.[89,90] The frontier orbitals for the group-15 hydrides in the D_{3h} arrangement are collected in Table V. These data show that the highest occupied molecular orbital (HOMO) a_2'' orbital energy is increasing from NH_3 to BiH_3. This a_2'' orbital is mainly responsible for the second-order JT distortion because it mixes with the unoccupied a_1' orbital, also shown in Table V. The difference in orbital energies $\Delta\epsilon = |\epsilon^{occ}(a_2'') - \epsilon^{unocc}(a_1')|$ decreases from NH_3 to BiH_3, and therefore the second-order JT distortion is expected to increase within this series.[91] The a_2'' orbital energies for SbH_3 and BiH_3 are similar and we cannot explain the sudden increase in the BiH_3 barrier height compared to SbH_3 using this qualitative model. We should point out that the unusual T-shaped structures of most of the group-15 fluorides can also be explained through a second-order JT distortion involving e' with a_1' orbital mixing, as

TABLE V. HF orbital energies of the group-15 hydrides (in a.u.).

	Occupied			Unoccupied	
	a_1'	e'	a_2''	a_1'	e'
NH_3	−1.127	−0.653	−0.391	0.015	0.022
PH_3	−0.859	−0.574	−0.302	0.015	0.023
AsH_3	−0.840	−0.552	−0.288	0.012	0.021
SbH_3	−0.762	−0.523	−0.266	0.011	0.022
BiH_3 (R)	−0.800	−0.501	−0.254	0.004	0.022
BiH_3 (NR)	−0.696	−0.504	−0.258	0.011	0.022

this is the case for ClF_3.[89] The valence e' orbitals in the hydride series are, however, low lying energetically and this explains why the hydrides prefer a trigonal planar transition state instead of a T-shaped arrangement.

Dai and Balasubramanian[16] have shown by calculation that the inversion barrier of BiH_3 is unusually high compared with those of its lighter congeners, and they have assumed that this is due to relativistic effects. We investigated the transition state in more detail at the QCI level. As in the case for the other group-15 hydrides, the inversion barrier for BiH_3 goes through a trigonal planar (D_{3h}) arrangement with a slightly shorter Bi–H bond length than that of the ground state, i.e., 1.735 Å for the D_{3h} structure at the relativistic QCI level. Figure 6 demonstrates that BiH_3 has no second transition state at a T-shaped arrangement at neither the nonrelativistic nor the relativistic level of theory. The QCI inversion barrier E_a is calculated to be 270.6 kJ/mol at the relativistic level and 189.0 kJ/mol at the nonrelativistic level. Hence, the unusually large inversion barrier of BiH_3 is indeed a relativistic effect. Is this due to the relativistic 6s contraction, which often is related to the inert pair effect?[16,86] The inversion process $C_{3v} \rightarrow D_{3h} \rightarrow C_{3v}$ is usually explained as a change in hybridization, $sp^3 \rightarrow sp^2 \rightarrow sp^3$. Hence, one may expect more s and less p involvement in the M–H bond at the D_{3h} transition state compared to the C_{3v} ground state. Indeed, a Mulliken population analysis shows a large increase in the p_z orbital populations for all compounds changing from the C_{3v} to the D_{3h} structure (Table VI). Relativistically frozen 6s electrons may hamper this process resulting in an increased activation barrier. As shown in Table VI, the Mulliken population analysis for the transition state shows a lower value of the 6s population, $n_s = 1.38$ at the RMP2 level and $n_s = 1.16$ at the NRMP2 level. This may indicate that the relativistically increased inertness of the $6s^2$ electron pair is responsible for the high activation barrier in BiH_3.

TABLE VI. HF and MP2 Mulliken orbital populations n_s, n_{p_z}, and n_p (total p population) and gross metal charges q for the group-15 hydrides. T denotes the trigonal planar transition state. The C_3 axis is defined in z direction.

		HF				MP2			
		n_s	n_{p_z}	n_p	q	n_s	n_{p_z}	n_p	q
NH_3		1.68	1.72	3.87	−0.58	1.66	1.70	3.87	−0.58
	T	1.43	1.87	4.16	−0.61	1.41	1.84	4.16	−0.60
PH_3		1.59	1.36	2.91	0.37	1.63	1.29	2.93	0.29
	T	1.38	1.89	3.50	0.02	1.37	1.86	3.50	0.00
AsH_3		1.56	1.28	2.83	0.50	1.57	1.22	2.87	0.38
	T	1.30	1.90	3.43	0.19	1.33	1.86	3.45	0.11
SbH_3		1.46	1.20	2.42	1.05	1.51	1.15	2.48	0.92
	T	1.17	1.92	3.11	0.69	1.20	1.88	3.11	0.62
BiH_3 (R)		1.67	1.03	2.20	1.19	1.71	0.99	2.28	1.04
	T	1.32	1.92	3.03	0.73	1.38	1.88	3.01	0.66
BiH_3 (NR)		1.54	1.15	2.29	1.30	1.59	1.11	2.27	1.17
	T	1.12	1.93	2.98	0.97	1.16	1.89	2.98	0.89

REX calculations show that the relativistic change of the MH_3 inversion barriers increases roughly as Z^2 and reaches about 40% for M = Bi. This is the first explicit estimate of the importance of relativistic effects on inversion barriers.[17] A Walsh diagram for REX/EHT orbital energies shows that the a_1 HOMO is the orbital whose energy increases with the angle α. The three lower energy levels suffer a slight decrease. This agrees with Dixon and Arduengo.[9-13] The spin–orbit averaged (QR) value for BiH_3 in Table VII is very close to the REX one, suggesting that the spin–orbit effects are not important. In fact, the relativistic 6p param-

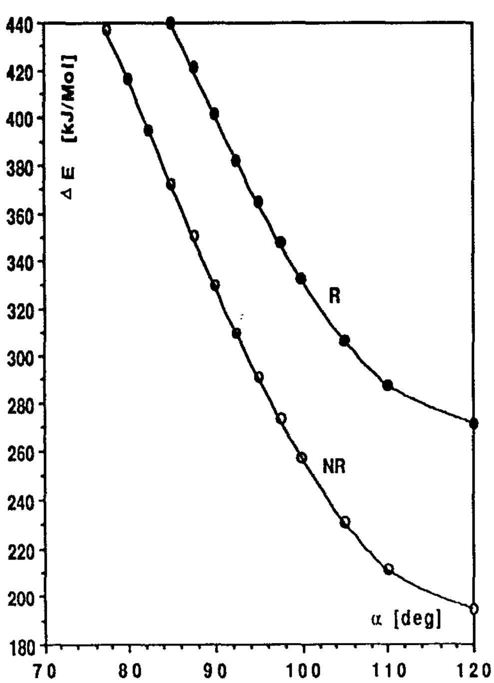

FIG. 6. Nonrelativistic and relativistic HF angle bending potential curves $\Delta E(\alpha)$ for planar BiH_3.

TABLE VII. Calculated inversion barriers E_a in kJ/mol and their relativistic changes $C = [E_a(R) - E_a(\mathrm{NR})]/E_a(\mathrm{NR})$ in percent. For the REX and EHT parameters, see text.

	E_a					
	Nonrelativistic		Relativistic		C	
Molecule	EHT	MP2	REX	MP2	REX	PP
NH_3	19	25	19	···	0.0	
PH_3	37	147	38	···	2.2	
AsH_3	75	164	80	···	7.2	
SbH_3	124	···	143	184	14.8	
BiH_3	151	187	211	264	40.4	41.6
			215[a]			
			222[b]			
			201[c]			
			150[d]			

[a]QR 6p.
[b]NR 6p.
[c]NR α_{6s}.
[d]NR ζ_{6s}.

TABLE VIII. HF and MP2 parameters for formula (1) using $x = \gamma - 180°$. Energy in kJ/mol and angle in degrees. The values in parentheses are defined as follows: $x(y)$ denotes $x \times 10^y$.

Molecule	Method	a	b	c	d
NH_3	HF	2.200(1)	− 9.790(− 2)	1.089(− 4)	2.582(− 4)
	MP2	2.510(1)	− 1.024(− 1)	1.045(− 4)	1.481(− 3)
PH_3	HF	1.323(2)	− 2.804(− 1)	1.486(− 4)	6.188(− 4)
	MP2	1.280(2)	− 2.460(− 1)	1.182(− 4)	5.572(− 4)
AsH_3	HF	1.711(2)	− 3.321(− 1)	1.611(− 4)	7.829(− 4)
	MP2	1.640(2)	− 2.904(− 1)	1.286(− 4)	7.035(− 4)
SbH_3	HF	1.925(2)	− 3.660(− 1)	1.740(− 4)	9.125(− 4)
	MP2	1.835(2)	− 3.212(− 1)	1.406(− 4)	8.327(− 4)
BiH_3 (NR)	HF	1.948(2)	− 3.702(− 1)	1.759(− 4)	1.035(− 3)
	MP2	1.865(2)	− 3.306(− 1)	1.465(− 4)	9.729(− 4)
BiH_3 (R)	HF	2.715(2)	− 4.855(− 1)	2.171(− 4)	1.647(− 3)
	MP2	2.642(2)	− 4.391(− 1)	1.824(− 4)	1.649(− 3)

eters can be replaced with nonrelativistic ones with little change in the barrier (footnote b, Table VII). Thus relativistic effects on the Bi 6s must cause the relativistic change of E_a. More precisely, its energetic stabilization (footnote c, Table VII) is not important, but its radial contraction (footnote d, Table VII) is. The effect of changing ζ_{6s} on the total energy (sum of the occupied orbital energies!) is small near the transition state and large at $\alpha = 90°$. Hence, as the a_1 HOMO is antibonding to the Bi 6s, its relativistic radial contraction relieves a part of this antibonding near equilibrium geometry, in the REX/EHT picture.

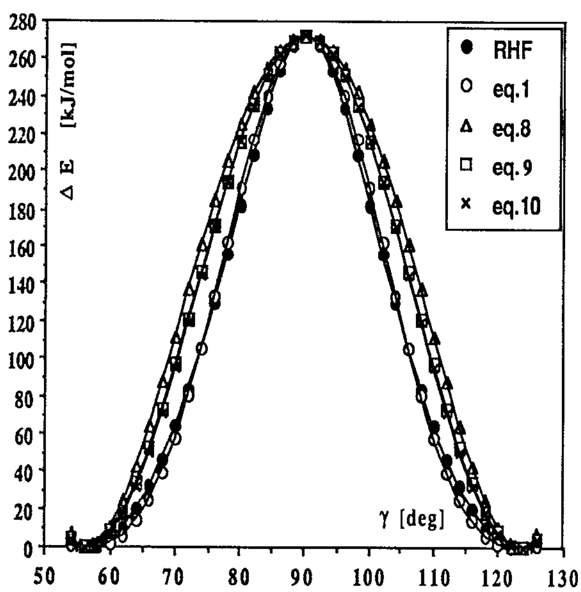

FIG. 7. Relativistic HF inversion potential curves for BiH_3 using Eqs. (1), (8), (9), and (10).

B. Tunneling frequencies and rates

The adjusted parameters for Eq. (1) are collected in Table VIII for both the HF and the MP2 approximation. Figure 7 shows the fit of Eq. (1) to calculated HF values for the relativistic BiH_3 inversion using as the tunneling coordinate $x = \gamma - 90°$. Figure 7 also includes other formulas which have been used in the past,[28,30]

$$V(\alpha) = A(\Delta\alpha)^2, \tag{9}$$

$$V(\gamma) = \tfrac{1}{2}E_a\{1 - \cos[180°(s - s_{\min})s_{\min}^{-1}]\}, \tag{10}$$

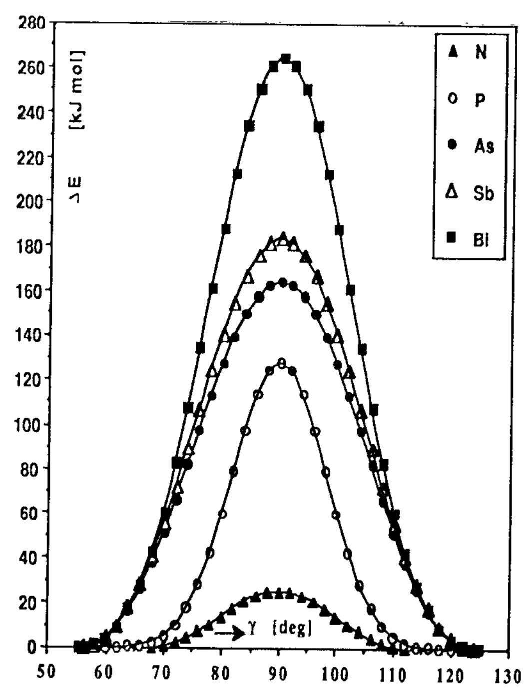

FIG. 8. MP2 inversion potential curves for the group-15 hydrides using Eq. (1) and the parameters given in Table VIII. The barrier height is monotonically increasing from NH_3 to BiH_3.

where $\Delta\alpha = (\alpha_{min} - \alpha)$ and α is the LML angle, A is an adjustable parameter for the barrier height E_a. γ and α (Fig. 1) are related through the well-known formula for C_{3v} symmetry, $\alpha = 2\sin^{-1}[\sin(180° - \gamma)\cos(30°)]$. Figure 7 shows that Eq. (1) is an excellent choice for the inversion potential curve. The deviations from the ideal curve are of some kJ/mol and within the range of error in the electron correlation and relativistic contributions. A comparison between the two curves of Eqs. (1) and (8) demonstrates that a simple polynomial fit may not be sufficient. Finally, in Fig. 8 we collect all inversion potentials for the group-15 hydrides which have been used for the numerical integration of integral I, Eq. (4).

The tunneling frequencies ν_T and rates $\tau_T = (2\nu_T)^{-1}$ are collected in Table IX. Note that the harmonic approximation has been used for both the HF and MP2 frequency

TABLE IX. HF and MP2 tunneling frequencies ν_T (in cm^{-1} and s^{-1}), tunneling rates τ_T (s) for the $\nu_2(A_1)$ bending mode, $\gamma(E_0)$ in degrees, and the integral I [Eq. (4)] in $(mol/g)^{1/2}$ for the MH_3 compounds (M = N to Bi) and ND_3 (D = deuterium). If not otherwise indicated, HF and MP2 refer to NRHF and NRMP2, respectively. Reduced masses ($\gamma = 90°$): NH_3, 2.4870; ND_3, 4.2006; PH_3, 2.7549; AsH_3, 2.9066; SbH_3, 2.9506; BiH_3, 2.9808. Experimental values from Refs. 76, 92, and 93. $x(y)$ denotes $x \times 10^y$. HO: zero-order harmonic-oscillator approximation (Ref. 94); P: four-order polynomial [Eq. (8)]; MSGB: modified symmetric Gaussian barrier, Eq. (1).

Molecule		Method	$\gamma(E_0)$	$I\ (mol/g)^{1/2}$	ν_T (cm^{-1})	ν_T (s^{-1})	τ_T
NH_3	HF	HO	···	···	8.081(−2)	2.423(+9)	2.064(−10)
		P	104.18	−3.231	2.189(0)	6.563(+10)	7.618(−12)
		MSGB	103.96	−3.169	2.413(0)	7.233(+10)	6.913(−11)
	MP2	HO	···	···	4.740(−2)	1.421(+9)	3.518(−10)
		P	105.58	−3.942	6.788(−1)	2.035(+10)	2.457(−11)
		MSGB	105.22	−3.897	7.289(−1)	2.185(+10)	2.288(−11)
		Expt.	···	···	7.935(−1)	2.379(+10)	2.102(−11)
ND_3	HF	HO	···	···	2.340(−3)	7.016(+7)	7.127(−9)
		P	105.17	−3.583	1.802(−1)	6.158(+9)	9.254(−11)
		MSGB	104.96	−3.519	2.045(−1)	5.403(+9)	8.119(−11)
	MP2	HO	···	···	1.720(−3)	5.156(+7)	9.697(−9)
		P	106.59	−4.315	3.714(−2)	1.114(+9)	4.490(−10)
		MSGB	106.45	−4.269	4.082(−2)	1.224(+9)	4.086(−10)
		Expt.	···	···	5.337(−2)	1.600(+9)	3.125(−10)
PH_3	HF	HO	···	···	7.750(−18)	2.323(−7)	2.152(+6)
		P	117.08	−23.226	6.329(−15)	1.897(−4)	2.635(+3)
		MSGB	116.15	−21.748	7.357(−14)	2.206(−3)	2.267(+2)
	MP2	HO	···	···	1.470(−18)	4.407(−8)	1.135(+7)
		P	118.49	−23.986	1.690(−15)	5.067(−5)	9.867(+3)
		MSGB	117.53	−22.479	2.061(−14)	6.179(−4)	8.092(+3)
AsH_3	HF	HO	···	···	4.269(−21)	1.280(−10)	3.907(+9)
		P	118.92	−29.966	2.085(−20)	6.250(−10)	8.000(+8)
		MSGB	117.73	−27.488	1.425(−18)	4.272(−8)	1.170(+7)
	MP2	HO	···	···	2.095(−21)	6.281(−11)	7.960(+9)
		P	120.35	−30.649	6.069(−21)	1.819(−10)	2.749(+9)
		MSGB	119.12	−28.161	4.224(−19)	1.266(−8)	3.949(+7)
SbH_3	RHF	HO	···	···	6.170(−25)	1.850(−14)	2.703(+13)
		P	119.96	−36.226	2.713(−25)	8.134(−15)	6.147(+13)
		MSGB	118.26	−32.781	1.009(−25)	3.024(−12)	1.653(+11)
	RMP2	HO	···	···	6.245(−24)	1.872(−14)	2.671(+13)
		P	120.90	−36.902	7.849(−26)	2.353(−15)	2.125(+14)
		MSGB	119.53	−33.439	3.007(−23)	9.015(−13)	5.546(+11)
BiH_3	HF	HO	···	···	7.200(−27)	2.158(−16)	2.316(+15)
		P	119.77	−39.570	5.554(−28)	1.665(−17)	3.003(+16)
		MSGB	118.29	−35.391	7.557(−25)	2.266(−14)	2.207(+13)
	MP2	HO	···	···	1.697(−26)	5.089(−16)	9.826(+14)
		P	120.86	−40.089	2.096(−28)	6.282(−18)	7.958(+16)
		MSGB	119.35	−35.849	3.171(−25)	9.505(−15)	5.260(+13)
BiH_3	RHF	HO	···	···	1.363(−28)	4.086(−18)	1.224(+17)
		P	121.11	−47.864	3.434(−34)	1.029(−23)	4.857(+22)
		MSGB	118.65	−40.039	2.530(−28)	7.584(−18)	6.593(+16)
	RMP2	HO	···	···	8.949(−28)	2.683(−17)	1.864(+16)
		P	122.32	−49.034	4.138(−35)	1.241(−24)	4.031(+23)
		MSGB	119.63	−40.578	9.064(−29)	2.717(−18)	1.840(+17)

splittings within the WKB approximation. The angles $\gamma(E_0)$ differ from $\gamma_{\min}$ by about 4°–8° depending on the element M. There is, however, a decreasing trend in this difference with increasing barrier height. For NH_3 the experimental $0^+/0^-$ ν_2 tunneling splitting is known ($\nu_T = 0.793$ cm^{-1}),[76,92,93] which compares extremely well with our calculated MP2 value ($\nu_T = 0.729$ cm^{-1}). However, the tunneling frequencies are sensitive to small changes in the molecular properties. For example, if we apply the experimental data listed in Table I ($\nu_0 = 886$ cm^{-1}, $r_e = 1.012$ Å, $\gamma_e = 112.14°$, $E_a = 24.2$ kJ/mol) which include anharmonicity effects, we obtain a smaller frequency splitting of $\nu_T = 0.486$ cm^{-1}.[95] This is still in satisfying agreement with the experimental value. The angle dependence of the reduced mass may be neglected, i.e., $\mu(\gamma) = \mu$ in Eq. (6) for all angles γ yields $\nu_T = 0.737$ cm^{-1} for NH_3 at the MP2 level. Also, the effect of constant bond length ($r = r_e$) in Eq. (7) for all angles γ changes the results only slightly, i.e., applying $r = r_e = 1.011$ Å for NH_3 at the MP2 level yields $\nu_T = 0.717$ cm^{-1}. Table IX demonstrates that a simple polynomial fit [Eq. (8)] for the inversion potential can lead to substantial errors in the tunneling frequencies. This is especially the case for the hydrides of the heavier elements. Hence, the results are sensitive to the potential ansatz chosen (see Fig. 7 for BiH_3) and this explains the large differences in published tunneling rates for PH_3 or AsH_3.[28,30,62] However, Fig. 7 leads to the assumption that our potential form (1) is accurate and therefore, the tunneling rates should be reasonably good.

Except for NH_3 the tunneling frequencies for the ground-state vibrational level are too small to be detected experimentally (even with ultrahigh-resolution spectroscopy), in contrast to earlier conclusions.[23,93] For example, Di-Lonardo and Fusina[80] did not observe any frequency splitting in the ν_2 bending mode of AsH_3 claiming a resolution of 0.006 cm^{-1}. Figure 9 collects the MP2 tunneling rates for all molecules on a logarithmic scale. There is a relatively smooth increasing trend in the tunneling rates from NH_3 (2×10^{-11} s) to BiH_3 (6×10^9 years). Clearly, relativistic effects change the tunneling rate of BiH_3 by orders of magnitude, as expected from the relativistic increase in the barrier height.

The inversion potentials [Eq. (1)] can be used for calculating tunneling splittings in excited vibronic states. For example, taking the published value of $\Delta\nu = 1\nu_2 - 0\nu_2 = 950$ cm^{-1} for the difference of the ground and first excited vibronic state of the H–N–H bending mode we obtain $\nu_T = 43.2$ cm^{-1} for the $1^+/1^-$ ν_2 levels (using the MP2 inversion potential and experimental frequencies) in very good agreement with the measured frequency splitting ($\nu_T = 36$ cm^{-1}).[56] Maki, Sams, and Olson[96] concluded from vibrational studies on PH_3 that the excited $4\nu_2$ level is split by less than their achieved resolution of 0.02 cm^{-1}. This agrees with our finding, i.e., using $E(4\nu_2) = 4375$ cm^{-1},[55] we obtain a tunneling splitting of $\nu_T = 1.2\times10^{-5}$ cm^{-1} which could be measured by ultrahigh-resolution spectroscopy (compare to the lower values of Spirko, Stone, and Papousek,[61] $\nu_T = 3\times10^{-10}$ cm^{-1}, or Civis, Carsky, and Spirko,[97] $\nu_T = 1.6\times10^{-7}$ cm^{-1}).

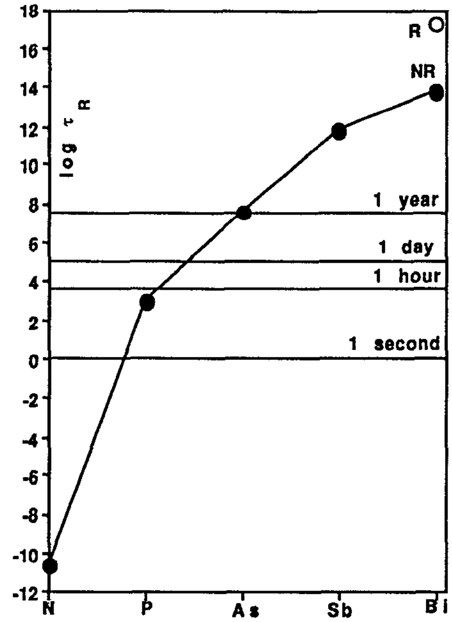

FIG. 9. Logarithmic curve for the MP2 tunneling rates τ_R of the group-15 hydrides.

If we assume that ND_3 follows the same inversion potential as NH_3 (compare, for example, the molecular properties for ND_3 and NH_3 published by Papousek and Spirko[55]), we obtain the values listed in Table IX. Our calculated MP2 value (4.08×10^{-2} cm^{-1}) is in excellent agreement with the experimental value (5.34×10^{-2} cm^{-1}). Table IX also includes the calculated data using a first-order harmonic-oscillator approximation published by Harmony.[94] This formula is easy to use since it contains only the properties ν_0 and $\gamma_{\min}$ for a molecule and is not dependent on the barrier height E_a or the shape of the inversion potential. This formula, however, does not perform very well even for very small tunneling frequencies and the agreement with experimental values obtained earlier for the NH_3 molecule[94] seems to be fortuitous. This is mainly so because Harmony's qualitative formula is very sensitive to small changes in ν_0 and $\gamma_{\min}$.

IV. CONCLUSION

HF and MP2 calculations for the inversion process of the group-15 hydrides have been performed. A modified one-dimensional symmetric Gaussian barrier has been introduced in order to calculate tunneling rates and frequencies for all molecules, which should be useful for a wider range of applications (see, for example, Ref. 98) where a one-dimensional potential curve is sufficient to describe the inversion of a molecule. The results obtained are in good agreement with experiment. This gives some confidence in the harmonic one-dimensional WKB approach for inversion tunneling. There have been, however, multidimensional approaches in order to calculate vibronic states of NH_3, which gave good results on the tunneling frequency ν_T for the $0\nu_2$ level despite the fact that only a SCF hypersurface was used.[99] The tunneling splitting in the $4\nu_2$ vibronic state of PH_3 may be large enough to be observed by ultrahigh-resolution spectroscopy. REX calculations suggest that the relativistic, radial 6*s* contraction causes the large relativistic increase of the BiH_3 inversion barrier. The monotonic increase in the inversion barriers from NH_3 towards BiH_3 can be explained qualitatively by a second-order Jahn–Teller distortion.

ACKNOWLEDGMENTS

The computer service and time given by the Center of Information Science and the IBM New Zealand Ltd. in Auckland, as well as the Australian National University Supercomputer Facility in Canberra are gratefully acknowledged. The author is very grateful to Professor Michael J. Taylor, Professor Martin A. Bennett, Dr. Graham A. Heath, and Dr. Mark McGrath for many valuable discussions.

[1] J. B. Lambert, in *Topics in Stereochemistry*, edited by N. L. Allinger and E. L. Eliel (Wiley, New York, 1971), Vol. 6.
[2] R. D. Baechler, J. D. Andose, J. Stackhouse, and K. Mislow, J. Am. Chem. Soc. **94**, 8060 (1972).
[3] C. C. Levin, J. Am. Chem. Soc. **97**, 5649 (1975).
[4] W. Cherry and N. Epiotis, J. Am. Chem. Soc. **98**, 1135 (1976).
[5] R. E. Weston, J. Am. Chem. Soc. **76**, 2645 (1954).
[6] J. D. Swalen and J. A. Ibers, J. Chem. Phys. **36**, 1914 (1962).
[7] R. Maripuu, I. Reineck, H. Ågren, W. Nian-Zu, J. Ming-Rong, H. Veenhuizen, S. H. Al-Shamma, L. Karlsson, and K. Siegbahn, Mol. Phys. **48**, 1255 (1983).
[8] A. Clotet, J. Rubio, and F. Illas, J. Mol. Struct. (Theochem) **164**, 351 (1988).
[9] D. A. Dixon, A. J. Arduengo, and T. Fukunaga, J. Am. Chem. Soc. **108**, 2461 (1986).
[10] D. A. Dixon, A. J. Arduengo, and D. C. Roe, J. Am. Chem. Soc. **108**, 6821 (1986).
[11] D. A. Dixon and A. J. Arduengo, J. Am. Chem. Soc. **109**, 338 (1987).
[12] D. A. Dixon and A. J. Arduengo, J. Chem. Soc., Chem. Commun. 498 (1987).
[13] D. A. Dixon and A. J. Arduengo, Int. J. Quantum Chem., Quantum Chem. Symp. **22**, 85 (1988).
[14] A. J. Arduengo and D. A. Dixon, in *Heteroatom Chemistry*, edited by E. Block (VCH, New York, 1990), pp. 47–77.
[15] Dai and Balasubramanian reported relativistic barriers assuming D_{3h} symmetry for the transition states of the As, Sb, and Bi hydrides (Ref. 16).
[16] D. Dai and K. Balasubramanian, J. Chem. Phys. **93**, 1837 (1990).
[17] L. J. Laakkonen, M. Sc. thesis, University of Helsinki, 1988 (unpublished).
[18] F. Bernardi, A. Bottoni, M. Olivucci, and G. Tonachini, J. Mol. Struct. (Theochem) **133**, 243 (1985).
[19] W. Cherry, N. Epiotis, and W. T. Borden, Acc. Chem. Res. **10**, 167 (1977).
[20] C. A. Jolly, F. Chan, and D. S. Marynick, Chem. Phys. Lett. **174**, 320 (1990).
[21] A. I. Boldyrev and O. P. Charkin, Zh. Strukt. Khim. **26**(3), 158 (1985).
[22] J. F. Liebman, P. Politzer, and W. A. Sanders, J. Am. Chem. Soc. **98**, 5115 (1976).
[23] W. Cherry, N. Epiotis, and W. T. Borden, Acc. Chem. Res. **10**, 167 (1977).
[24] A. Rauk, L. C. Allen, and K. Mislow, Angew. Chem. Int. Ed. Engl. **9**, 400 (1970).
[25] P. Schwerdtfeger (unpublished).
[26] R. A. Eades and D. A. Dixon, J. Chem. Phys. **72**, 3309 (1980).
[27] D. A. Dixon and D. S. Marynick, J. Am. Chem. Soc. **99**, 6101 (1977).
[28] C. C. Costain and G. B. B. M. Sutherland, J. Phys. Chem. **56**, 321 (1952).
[29] R. P. Bell, *The Tunnel Effect in Chemistry* (Chapman and Hall, London, 1980).
[30] R. S. Berry, J. Chem. Phys. **32**, 933 (1960).
[31] G. B. B. M. Sutherland, E. Lee, and C. K. Lu, Trans. Faraday Soc. **35**, 1373 (1939).
[32] P. Pyykkö, in *Methods in Computational Chemistry*, edited by S. Wilson (Plenum, New York, 1988), Vol. 2, pp. 137–226.
[33] P. Pyykkö and L. L. Lohr, Inorg. Chem. **20**, 1950 (1981); see Table A (supplementary material). The same parameters are included in QCPE 387 and 468. The quasirelativistic (QR) average parameters for Bi 6*p* are $\alpha = -7.808$ eV and $\zeta = 2.139$.
[34] An $\alpha_H = -13.6$ eV was also tested. Although it gives exaggerated ionicity and higher barriers, the (percental) relativistic barrier change was closely similar.
[35] K. S. Krasnov, *Molecular Constants of Inorganic Compounds* (in Russian) (Khimiya, Leningrad, 1979).
[36] M. J. Frisch, M. Head-Gordon, H. B. Schlegel, K. Raghavachari, J. S. Binkley, C. Gonzales, D. J. DeFrees, D. J. Fox, R. A. Whiteside, R. Seeger, C. F. Melius, J. Baker, R. Martin, L. R. Kahn, J. J. P. Stewart, E. M. Fluder, S. Topiol, and J. A. Pople, program GAUSSIAN88, Gaussian Inc., Pittsburgh, PA, 1988.
[37] R. Ahlrichs, M. Häser, C. Kölmel, H. Horn, and M. Baer, program TURBOMOLE, University of Karlsruhe, 1988.
[38] M. Häser and R. Ahlrichs, J. Comput. Chem. **10**, 104 (1989).
[39] R. Ahlrichs, M. Baer, M. Häser, H. Horn, and C. Kölmel, Chem. Phys. Lett. **162**, 165 (1989).
[40] J. A. Pople, M. Head-Gordon, and K. Raghavachari, J. Chem. Phys. **87**, 5968 (1987).
[41] J. Paldus, J. Cizek, and B. Jeziorski, J. Chem. Phys. **90**, 4356 (1989); **93**, 1485 (1990).
[42] K. Raghavachari, M. Head-Gordon, and J. A. Pople, J. Chem. Phys. **93**, 1486 (1990).
[43] J. A. Pople, M. Head-Gordon, D. J. Fox, and K. Raghavachari, J. Chem. Phys. **90**, 5622 (1989).
[44] S. Huzinaga, J. Chem. Phys. **42**, 1293 (1965).
[45] G. C. Lie and E. Clementi, J. Chem. Phys. **60**, 1275 (1974).
[46] G. W. Trucks, J. D. Watts, E. A. Salter, and R. J. Bartlett, Chem. Phys. Lett. **153**, 490 (1988).
[47] R. Poirier, R. Kari, and I. G. Csizmadia, *Handbook of Gaussian Basis Sets*, Vol. 24 in Physical Sciences Data (Elsevier, Amsterdam, 1984).
[48] R. C. Binning and L. A. Curtiss, J. Chem. Phys. **92**, 1860 (1990).
[49] G. Igel-Mann, H. Stoll, and H. Preuss, Mol. Phys. **65**, 1321 (1988).
[50] W. Küchle, M. Dolg, H. Stoll, and H. Preuss, Mol. Phys. **74**, 1245 (1991).
[51] S. Huzinaga, J. Andzelm, M. Klobukowski, E. Radzio-Andzelm, Y. Sakai, and H. Tatewaki, *Gaussian Basis Sets for Molecular Calculations*, Vol. 16 in Physical Sciences Data (Elsevier, Amsterdam, 1984).
[52] E. B. Wilson, J. C. Decius, and P. C. Cross, *Molecular Vibrations* (McGraw-Hill, London, 1955).
[53] P. Schwerdtfeger, G. A. Bowmaker, P. D. W. Boyd, C. D. Earp, and S. F. Hannon, program VIB, version 7.1, University of Auckland, Department of Chemistry, Auckland, 1991.
[54] D. M. Dennison and G. E. Uhlenbeck, Phys. Rev. **41**, 313 (1932).
[55] D. Papousek and V. Spirko, Topics Current Chem. **68**, 59 (1976).
[56] C. H. Townes and A. L. Schawlow, *Microwave Spectroscopy* (McGraw-Hill, New York, 1955).
[57] J. E. Wollrab, *Rotational Spectra and Molecular Structure* (Academic, New York, 1967).
[58] M. F. Manning, J. Chem. Phys. **3**, 136 (1935).
[59] S. I. Chan, J. Zinn, J. Fernandez, and W. D. Gwinn, J. Chem. Phys. **33**, 1643 (1960).
[60] G. Campoy, A. Palma, and L. Sandoval, Int. J. Quantum Chem., Quantum Chem. Symp. **23**, 355 (1989).
[61] V. Spirko, J. M. R. Stone, and D. Papousek, J. Mol. Spectrosc. **60**, 159 (1976).
[62] V. Spirko, J. M. R. Stone, and D. Papousek, Mol. Phys. **36**, 791 (1978).
[63] K. H. Hellwege, *Landolt-Börnstein, Zahlenwerte und Funktionen aus Naturwissenschaften und Technik* (Springer, Berlin, 1976), Vol. 7.
[64] A. L. McClellan, *Tables of Experimental Dipole Moments* (Freeman, San Francisco, 1963).
[65] E. D. Simandiras, N. C. Handy, and R. D. Amos, J. Chem. Phys. **88**, 3174 (1988).
[66] W. R. Rodwell and L. Radom, J. Chem. Phys. **72**, 2205 (1980).
[67] W. R. Rodwell and L. Radom, J. Am. Chem. Soc. **103**, 2865 (1981).

[68] R. M. Stevens, J. Chem. Phys. **55**, 1725 (1971).
[69] R. M. Stevens, J. Chem. Phys. **61**, 2086 (1974).
[70] R. Ahlrichs, F. Driessler, H. Lischka, V. Staemmler, and W. Kutzelnigg, J. Chem. Phys. **62**, 1235 (1975).
[71] R. Ahlrichs, F. Keil, H. Lischka, W. Kutzelnigg, and V. Staemmler, J. Chem. Phys. **63**, 455 (1975).
[72] D. S. Marynick and D. A. Dixon, J. Phys. Chem. **86**, 914 (1982).
[73] G. E. Scuseria, A. C. Scheiner, J. E. Rice, T. J. Lee, and H. F. Schaefer, Int. J. Quantum Chem., Quantum Chem. Symp. **21**, 495 (1987).
[74] K. F. Freed, Chem. Phys. Lett. **2**, 255 (1968).
[75] C. A. Jolly, F. Chan, and D. S. Marynick, Chem. Phys. Lett. **174**, 320 (1990).
[76] W. S. Benedict and E. K. Plyler, Can. J. Phys. **35**, 1235 (1957).
[77] G. Tarrago, M. Dang-Nhu, and A. Goldman, J. Mol. Spectrosc. **88**, 311 (1981).
[78] A. Baldacci, V. M. Devi, and K. N. Rao, J. Mol. Spectrosc. **81**, 179 (1980).
[79] K. Nakamoto, *Infrared and Raman Spectra of Inorganic and Coordination Compounds*, 4th ed. (Wiley, New York, 1986).
[80] G. DiLonardo and L. Fusina, J. Mol. Spectrosc. **104**, 282 (1984).
[81] T. Koops, T. Visser, and W. M. A. Smit, J. Mol. Struct. **96**, 203 (1983).
[82] D. E. C. Corbridge, Top. Phosphorus Chem. **6**, 235 (1969).
[83] E. Lee and C. K. Wu, Trans. Faraday Soc. **35**, 1366 (1939).
[84] R. D. Amos, J. Chem. Soc. Faraday Trans. **83**, 1595 (1987).
[85] M. Dolg, W. Küchle, H. Stoll, H. Preuss, and P. Schwerdtfeger, Mol. Phys. **74**, 1265 (1991).
[86] P. Schwerdtfeger, G. A. Heath, M. Dolg, and M. A. Bennett, J. Am. Chem. Soc. (submitted).
[87] S. Nordholm, Aust. J. Chem. **40**, 1465 (1987).
[88] R. Ahlrichs, Chem. Unserer Zeit **14**, 18 (1980).
[89] J. K. Burdett, Chem. Soc. Rev. 507 (1978).
[90] C. Edmiston, J. Jarvie, and J. Bartleson, J. Chem. Phys. **84**, 6907 (1986).
[91] This analysis should be taken with care since the virtual a_1' orbital concerned may be sensitive to basis-set effects. However, the a_2'' HOMOs show a clear trend of increasing orbital energy from NH_3 to BiH_3.
[92] D. M. Hirst, *Potential Energy Surfaces* (Taylor & Francis, London, 1985).
[93] D. Papousek and M. R. Aliev, *Molecular Vibrational-Rotational Spectra*, Vol. 17 in Studies in Physical and Theoretical Chemistry (Elsevier, Amsterdam, 1982).
[94] M. D. Harmony, Chem. Phys. Lett. **10**, 337 (1971).
[95] We took the parameters $d = 1.481 \times 10^{-3}$ from the MP2 calculation and chose $a = 24.20$, $b = -0.098\,74$, and $c = 1.007 \times 10^{-4}$.
[96] A. G. Maki, R. L. Sams, and W. B. Olson, J. Chem. Phys. **58**, 4502 (1973).
[97] S. Civis, P. Carsky, and V. Spirko, J. Mol. Spectrosc. **118**, 88 (1986).
[98] R. A. Eades, D. A. Weil, D. A. Dixon, and C. H. Douglass, Jr., J. Phys. Chem. **85**, 976 (1981).
[99] N. Shida, J. E. Almlöf, and P. F. Barbara, Theor. Chim. Acta **76**, 7 (1989).